Available online at www.sciencedirect.com
ScienceDirect
European Journal of Mechanics B/Fluids 25 (2006) 621–635

Nonlinear analysis and simulations of measured freak wave time series

Alexey Slunyaev *

Institute of Applied Physics, RAS, 46, ul. Ulyanova, GSP-120, Nizhny Novgorod, 603905, Russia

Received 11 October 2005; received in revised form 27 December 2005; accepted 23 March 2006

Available online 22 May 2006

Abstract

The analysis of surface waves time series is performed to understand the nature of freak waves. Contributions of quasi-linear dispersive focusing effects and nonlinear self-modulation (Benjamin–Feir) effects are estimated with the help of kinematical description, nonlinear spectral analysis and numerical simulations. The nonlinear dynamics of an envelope soliton over a background wave is investigated and a possible extreme wave appearance is predicted.

Keywords: Freak waves; Surface wave analysis; Inverse scattering transform

1. Introduction

The appropriate estimation of possible extreme wave heights, shapes and statistics is requested due to the evidence of freak wave phenomenon. It is vitally important to provide safe navigation, sea usage and firm ship and offshore constructions. Although the problem of freak waves got a stimulus to investigation not long ago, the measurements of wave movement have been conducted for decades; therefore some material for statistic analysis has been already obtained. Many-year wave recordings and hundreds (to our knowledge) of observed freak waves nevertheless cannot provide a single meaning to answer the question about the statistics of freak waves (compare, for instance, [1–3]). It may be caused by several reasons. Omitting the problems of measurements and approaches, we may cite different field conditions of measurements and statistically heterogeneous data.

Intensive numerical simulations of dynamical models may be performed to obtain numerous statistically homogeneous virtual records of freak waves. The data may be further processed, and this is the way to see the non-gaussianity of the surface wave probability density function and the influence of the wave spectrum on the frequency of freak wave occurrence. Such study has become very popular nowadays, and active research is being carried out in this direction [4–9]. The mathematical and numerical models of surface wave are rapidly improving as well as the power of computing machines. That is why this manner of obtaining physical results is promising.

* Tel.: +7 8312 164674; fax: +7 8312 365976.
E-mail address: Slunyaev@hydro.appl.sci-nnov.ru (A. Slunyaev).

0997-7546/$ – see front matter
doi:10.1016/j.euromechflu.2006.03.005

Nevertheless a clear idea about the mechanism of the freak wave occurrence should be assumed to have a numerical wave tank, which is adequate to the real ocean regarding the problem of freak waves. Different approximations and assumptions may be applied to build a simpler mathematical model. This leads to a different range of applicability and accuracy. If the role of this or that physical effect is misunderstood, the choice of the inadequate mathematical model is sure to kill all physical meaning of the results.

It would be a perfect achievement if one could predict the occurrence of a freak wave in a certain place at the given time, but unlikely seems realizable. It would have great practical importance if one could announce the most probable area and sea conditions for the freak wave formation. This is quite a realistic goal, and it may be gained either by searching and simulating all possible cases, or having an idea about the main cause of a freak wave formation. But how is it possible to determine this *main* mechanism (or these mechanisms) of a freak wave generation? To our mind, it could be done via detailed analysis of available instrumental registrations of freak waves, which could become the shortest way to understand the nature of the phenomenon.

We have analyzed several freak wave time series to estimate the role of two important effects in surface wave dynamics: dispersion focusing and nonlinear self-modulation (Benjamin–Feir instability). The first of the waves, the New Year Wave (Draupner platform, the North Sea) became famous after [10,11]; it was considered in [12,13]. Ten wave records were measured from the North Alwyn platform (the North Sea); four of them were studied in [14], six others were announced in [15] and will appear elsewhere. The latter freak wave was registered in the Black Sea, and was presented in [16]. In this paper the elaborated methods to make clear the dispersive and nonlinear effects are discussed, and some generalization of the conducted analyses is presented. Two records, namely, NA9711180110 and NA9711192011, measured from North Alwyn platform on November 18, 1997 01:10 and November 19, 1997 20:11 are used for illustrations.

2. Freak wave time series

A freak wave instrumental registration is typically represented by a 15–20 minute time series measured at a single point with some frequency of acquisition, which defines the discretization of the record. Often a freak wave is supposed to be the only huge wave among typical ones (see Fig. 1C), although it may be a part of intensive wave group, as it is seen on Fig. 2C. As the only criterion for a freak wave definition we use the amplitude one:

$$AI = H_{\mathrm{fr}}/H_{\mathrm{s}} > 2, \tag{1}$$

where H_{s} is the significant wave height. The abnormality index AI does not exceed 2.4 for the considered measurements from the North Sea and equals 3.9 for the Black Sea record, while the maximum known amplification registered at the North Alwyn [3] is equal to 3.2. Unfortunately the Black Sea time series has very poor discretization with the peak wave represented by a single point, and its abnormality index is doubtful, although other waves have good resolution.

All the records concerned correspond to deep water: $KD \approx 2$ for the New Year Wave, $3.6 < KD < 7.2$ for the time series from North Alwyn, and $KD \approx 9.6$ for the Black Sea record; where D is the depth of the place, and K is the currier wave number. The typical wave period is 6–12 s (this corresponds to wavelengths 60–230 meters), the averaged steepness of the time series does not exceed value 0.1 what proves relatively weakly nonlinear wave dynamics, although the peak steepness of the freak waves tends to the breaking limit 0.4 and may exceed it.

3. Local wave properties

A freak wave represents the exceptional wave among the field of usual (smaller) oceanic waves. That is why average characteristics of the waves may display the properties of the sea state, but not the rogue wave (and, apparently, of the way how it was formed). To get a better understanding of the processes local wave parameters may be considered. To obtain the local parameters intervals of several (say, three) wave periods within a sliding window are used after applying the Hanning data mask.

The mean frequency Ω is obtained in this way as first moment of Fourier spectral density. The example of this curve is given on Figs. 1 and 2 on panels A and B (the solid white line on the background of the Fourier time-frequency spectra) for two different durations of the sampling window T_{win}. It has some variation during the 20-minute record, which becomes more evident if expressed in terms of group velocity C_{gr} (see Figs. 1D and 2D). The deviation of

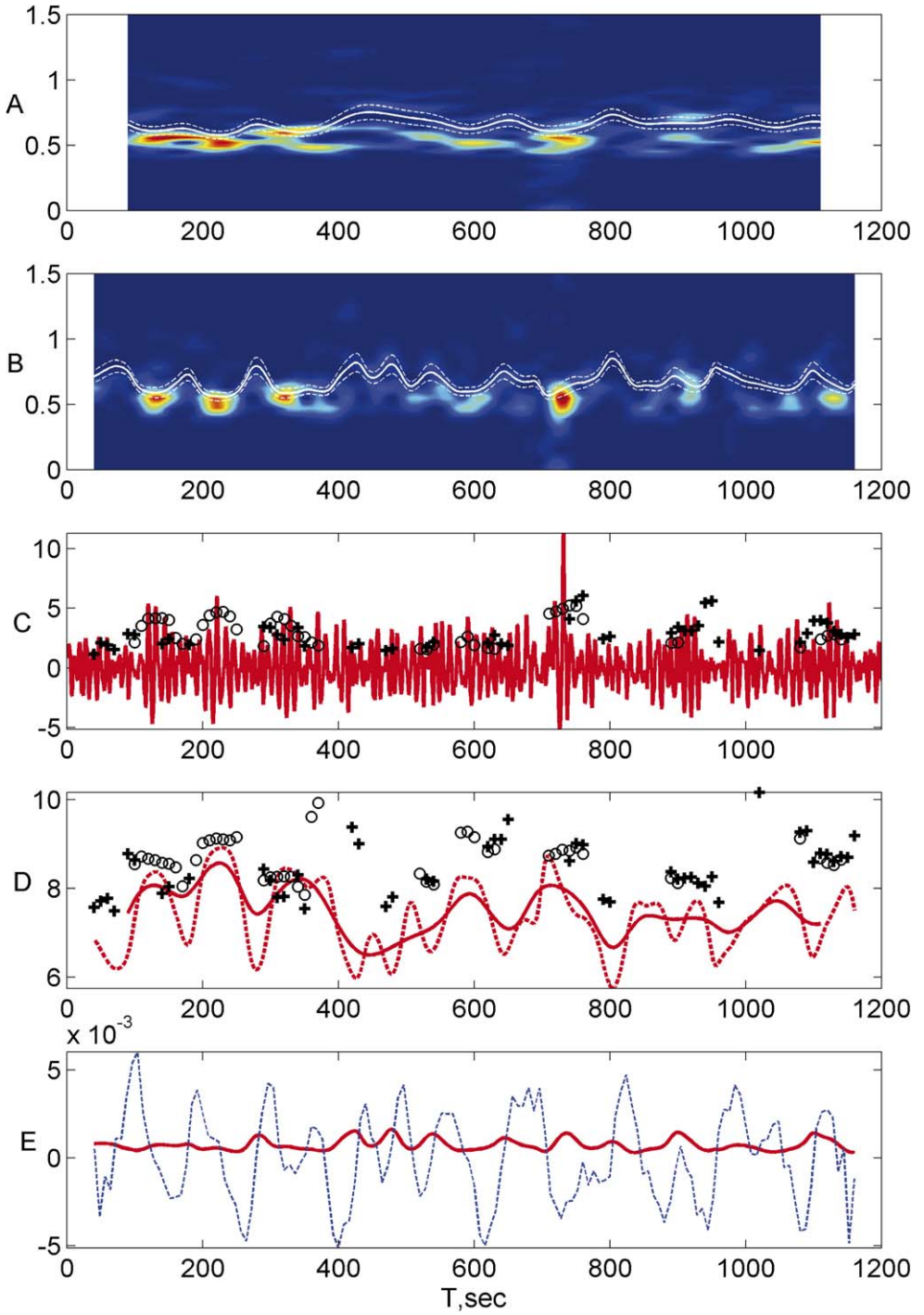

Fig. 1. Wave record NA9711180110. Panel A: time-frequency Fourier spectrum built for the sampling window of 117 s duration (about 10 wave periods); straight line shows the local mean frequency Ω_0, dashed lines bound the domain of Benjamin–Feir instability $\Omega_0 \pm \Omega_{\mathrm{BF}}$. Panel B: the same as on Panel A, but for the sampling window of 36 s duration (3 wave periods). Panel C: measured time series of the surface displacement (in meters). Symbols denote the determined amplitudes of solitary waves with permanent normalizing (circles) and flexible normalizing (crosses). Panel D: Local group velocities (in m/s) defined for the sampling window of 117 s (solid line) and 36 s (dashes). Symbols denote the determined velocities of solitary waves: permanent normalizing (circles) and flexible normalizing (crosses). Panel E: Growth rates σ_{BF} (solid) and σ_{dis} (dashed) (in s^{-1}) defined with the sampling window of 36 s.

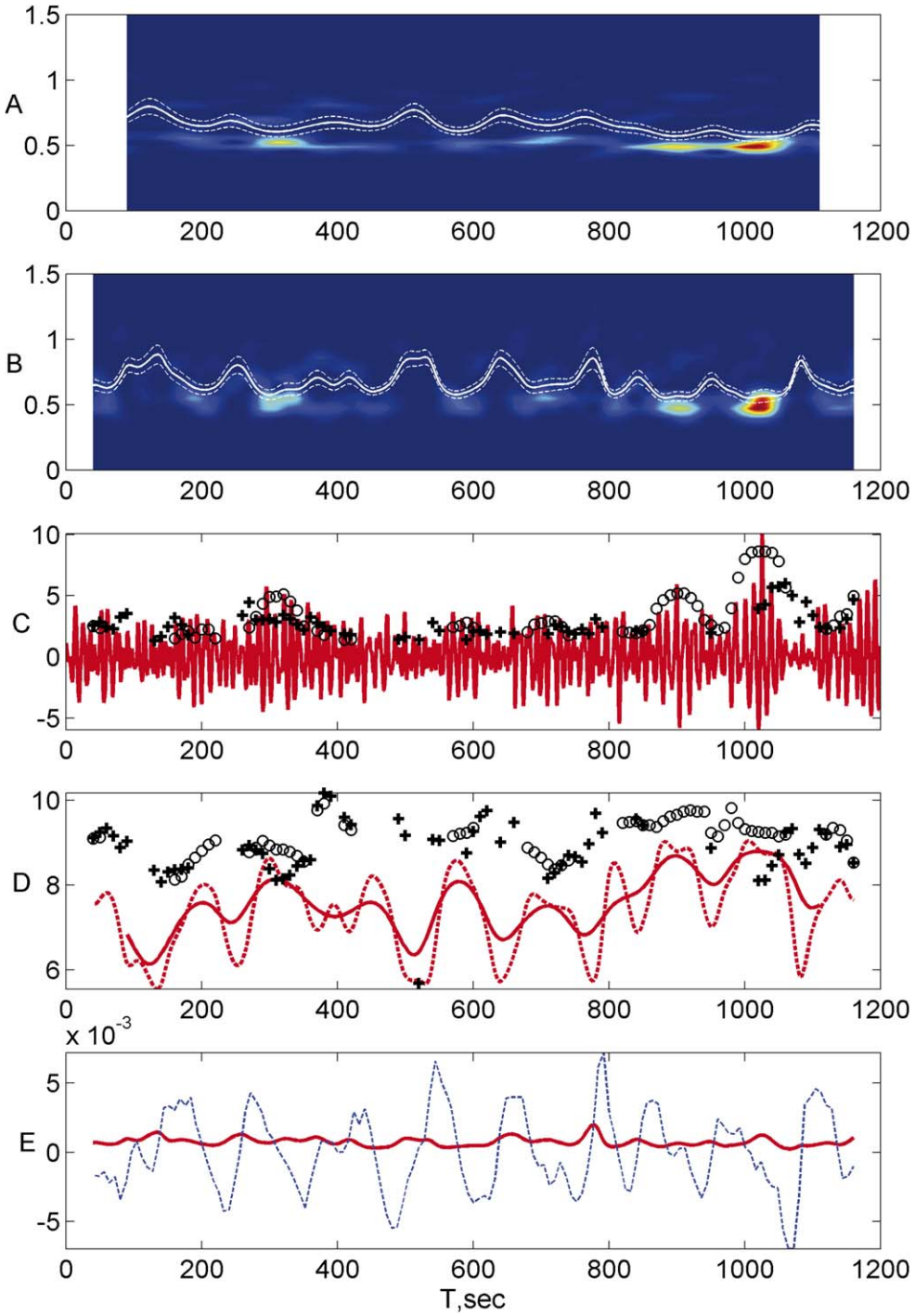

Fig. 2. Wave record NA9711192011. The contents of the panels is same as on Fig. 1.

the group velocities observed on the figures is about 50%; it leads to the energy exchange between the individual waves. This may provide the wave growth or decrease and represents the simplest case of dispersive focusing. For the simplest analysis of this process the kinematic theory may be used accompanied by the energy balance equation [17]

$$\frac{\partial C_{\mathrm{gr}}}{\partial T} + C_{\mathrm{gr}} \frac{\partial C_{\mathrm{gr}}}{\partial X} = 0, \qquad \frac{\partial \eta^2}{\partial T} + \frac{\partial}{\partial X}\left(C_{\mathrm{gr}} \eta^2\right) = 0 \tag{2}$$

where $\eta(X,T)$ is the surface elevation. Then the total derivative of the energy quantity is given by:

$$\frac{\mathrm{d}\eta^2}{\mathrm{d}T} = 2\sigma_{\mathrm{dis}}\eta^2, \qquad \sigma_{\mathrm{dis}} = \frac{1}{2C_{\mathrm{gr}}}\frac{\partial C_{\mathrm{gr}}}{\partial T}. \tag{3}$$

Parameter σ_{dis} expresses the exponential growth rate due to dispersive wave convergence. Waves grow when $\sigma_{\mathrm{dis}} > 0$ and vice versa. The dispersive growth rates computed for the time series are given on Figs. 1 and 2 (panel E, dashed lines).

The simplest nonlinear theory is based on of the nonlinear Schrodinger equation (NLS) [18]. In the assumption of unidirectional wave propagation Stokes waves become unstable due to the modulational (Benjamin–Feir, BF) instability for sufficiently deep water ($KD > 1.363$). This fact is represented by the instability of the exact solution of NLS – the plane wave. The focusing type of NLS equation may be written in the convenient dimensionless form for $q(x,t)$

$$\mathrm{i}q_x + q_{tt} + 2q|q|^2 = 0, \tag{4}$$

where

$$\eta = \frac{\sqrt{2}}{K}\,\mathrm{Re}\big[q\exp\big(\mathrm{i}(\Omega T - KX)\big)\big], \quad t = \Omega T - 2KX,\ x = KX.$$

Note, that Eq. (4) describes the evolution in space.

The exact solution of (4) – the plane wave $q_{\mathrm{pw}}(x,t) = \mathrm{e}^{2\mathrm{i}x}$ is known to be unstable with respect to long harmonic perturbations with frequency $\Delta\omega < \omega_{\mathrm{BF}}$, where $\omega_{\mathrm{BF}} = 1$, or in physical variables

$$2\frac{\Delta\Omega}{\Omega} = \frac{\Delta K}{K} < 2\sqrt{2}K\eta, \tag{5}$$

where $\Delta\Omega$ and ΔK are the frequency and the wave number of the wave perturbation. The unstable frequency domain $\Omega \pm \Omega_{\mathrm{BF}}$ is shown by dashed lines on Figs. 1, 2 (panels A). The initial stage of the modulational growth is described by the exponential law with maximum growth rate given by formula

$$\sigma_{\mathrm{BF}} = \frac{1}{2}\Omega K^2\eta^2. \tag{6}$$

The two growth rates σ_{dis} and σ_{BF} can be used for rough estimations of the time scales of dispersive and nonlinear wave focusing effects. It is seen from Figs. 1, 2 (panels E) that dispersion typically works faster, while estimated modulational growth should take more than 500 s.

It is worth remarking that although the NLS theory is valid for weakly nonlinear processes only, formally it may describe strong self-focusing effects. The nonlinearity is characterized by the dimensionless parameter $s = \eta K$, which is steepness, although the strength of self-focusing is characterized by so-called soliton number or Benjamin–Feir index, which may be expressed as

$$I_{\mathrm{BF}} = \sqrt{2}sn_t, \tag{7}$$

where $n_t = 2n_x$ are the numbers of individual waves contained in the wave packet (observed in a time and space series accordingly); they are inverse values of the relative spectral bandwidths ($n_t = \Omega/\Delta\Omega$). It follows from (5) that a plane wave is unstable if $I_{\mathrm{BF}} > 1$, what may happen if steepness s is small, but the wave group is sufficiently long (7 waves in a time series if $s \approx 0.1$). It is necessary to mention that although the BF index was originally suggested through statistical description of modulationally unstable waves aiming to take into account the finite spectral bandwidth, in the present paper this index is understood more in the "dynamical" sense (as the soliton number). We do not divide these two parameters hereafter, although one should bear this difference in mind.

4. Search for solitons

The estimation of the effects of nonlinear self-modulation on the basis of the stability criterion for a plane wave (or definition of the BF index by (7)) seems quite rough, since the usual sea waves are modulated in frequency and amplitude. One may consider the modulational instability as the manifestation of a nonlinear dynamics of localized solitary waves. When solitary waves interact with other waves, a beating may be observed which is a general case

of the modulational growth. The envelope soliton of the NLS equation is the first approximation for oceanic solitary groups. For the equation in form (4) the soliton solution is given by

$$q_{\rm sol}(x,t) = a_{\rm sol}\frac{\exp({\rm i}t/(2v_{\rm sol}) - {\rm i}x(1/(4v_{\rm sol}^2) - a_{\rm sol}^2))}{\cosh(a_{\rm sol}/v_{\rm sol})(x - v_{\rm sol}t)}. \tag{8}$$

Here $a_{\rm sol}$ and $v_{\rm sol}$ are dimensionless amplitude and velocity of the soliton; physical parameters (capital letters) are connected with the dimensionless ones (small letters) by

$$A = \frac{\sqrt{2}}{K}a, \qquad V = \frac{\Omega}{K(2+v^{-1})}; \tag{10}$$

the applicability of the NLS theory requires the quantity $|v^{-1}|$ being small. The envelope solitons in the frameworks of the NLS equation interact elastically with other waves preserving their energy. Fully numerical computations show that they may live quite long if the steepness is moderate (about 0.1) [19]. When envelope solitons interact with other waves, the wave field may look complicated; the possibility to detect the hidden solitons in the time series may provide an effective tool in comprehension and prediction nonlinear wave dynamics. This can be done with the help of the Inverse Scattering Technique, first applied for the focusing NLS equation in [20]. The solution of the associated linear scattering problem integrates the NLS equation. In the manner of AKNS [21] the scattering problem may be represented in form

$$\Psi_t = \begin{pmatrix} \lambda & q \\ -q^* & -\lambda \end{pmatrix}\Psi, \qquad \Psi = \begin{pmatrix} \psi_1 \\ \psi_2 \end{pmatrix}. \tag{11}$$

The spectrum of it does not change in time, and its discrete part specifies envelope solitons.

The direct scattering problem may be solved analytically for some cases of initial perturbations. In particular it is shown for some shapes of positive impulse-like disturbances that the number of generated solitons is defined by

$$N = \left[I_{\rm BF} + \frac{1}{2}\right], \tag{12}$$

where square brackets take the integer part of the inner expression. The BF index in (12) is defined in more general form

$$I_{\rm BF} = \pi^{-1}\int\limits_{-\infty}^{\infty} |q|\,{\rm d}t \tag{13}$$

and tends to (7) in the particular case of a perturbed plane wave.

The idea to seek solitons in a time series was, evidently, first realized in [22] for the shallow-water case, when the waves were described within the frameworks of Korteweg–de Vries equation. Recently similar technique has been used for the study of freak waves over deep water – within the NLS approach [23,24]. The way to use the scattering problem suggested in this paper differs in some important parts.

At first, the scattering problem for the infinite line is considered and only discrete spectrum is looked for, what simplifies the problem greatly if compared with periodical formulation. Then the parameters of solitons are simply related to the spectrum as

$$a_{\rm sol} = 2\,{\rm Re}\,\lambda \quad \text{and} \quad v_{\rm sol}^{-1} = 4\,{\rm Im}\,\lambda. \tag{14}$$

The solution of the inverse scattering problem requires the knowledge of the eigenmodes. But we do not reconstruct the wave field. The direct scattering problem is solved in a sliding sampling window of length $T_{\rm win}$ to identify the positions of solitons and to compensate the variation of the mean frequency within the record (which can strongly effect the spectrum λ due to the normalization (4) of the NLS equation).

The amplitudes of revealed solitons are plotted in circles and crosses on panels C of Figs. 1 and 2; corresponding soliton velocities are given on panels D. The circles denote the case when the mean frequency for each of the integrated intervals was supposed to be equal to the average within all the 20-min record (permanent normalization). The crosses correspond to the case of flexible normalization, when the mean frequency was obtained for each extract independently. It is evidently seen that sometimes the results may be rather different. After having a look at the curves

of group velocity (panel D), it becomes clear that a soliton vanishes if the mean group velocity increases. The effect of non-uniformity of modulated wave packets was considered by [25] and the same result was achieved: the BF instability is depressed when the local group velocity increases and is intensified when $C_{\rm gr}$ becomes smaller.

Only the first (most intensive) soliton defined in an extract is shown on the figures. Other determined solitons are usually much smaller and not very trustworthy. Although the revealed solitons can be often seen by eye (see Figs. 1, 2, panel C), they interact nonlinearly with other waves. Some estimations of the results of the above-mentioned interaction are concerned in the next section.

5. Interaction of a soliton envelope with background waves

The so-called 'breather' solutions of the NLS equation represent nonlinear interaction of an envelope soliton with a background plane wave. The breather-type solutions were first obtained in [26,27] and completed later [28,29]. A simplest case of a breather is represented by a single eigenvalue of the associated scattering problem in the case when the solution tends to a plane wave at infinity ($t \to \pm\infty$ for the case of the spatial version of the evolution equation (4)). Except different boundary conditions other details of the scattering problem are identical to the classical one given by (11). In this understanding a breather may be called a soliton (Kuznetsov–Ma soliton) or a superposition of a classical envelope soliton of NLS with a plane wave. Naturalness and richness of this interpretation will be shown below. We will use the general form of the solution of [26,27], obtained directly from the inverse scattering problem in [30]; for the equation in form (4) it is:

$$q_{\rm br}(x,t) = \mathrm{e}^{2\mathrm{i}x}\frac{\cos\eta\cos(2\gamma(x-wt)+2\mathrm{i}\psi)-\cosh\psi\cosh(2\Gamma(x-v_{\rm br}t)+2\mathrm{i}\eta)}{\cos\eta\cos(2\gamma(x-wt))-\cosh\psi\cosh(2\Gamma(x-v_{\rm br}t))}, \tag{15}$$

$$\Gamma = -\sinh\psi\cos\eta, \qquad \gamma = \cosh\psi\sin\eta,$$

$$v_{\rm br} = \Gamma^{-1}\cosh 2\psi\sin 2\eta, \qquad w = \gamma^{-1}\sinh 2\psi\cos 2\eta,$$

$$\lambda = \cos(\eta + \mathrm{i}\psi).$$

This solution with the help of the Hirota method was also found in [31]; it tends to a plane wave with unit amplitude $a_{\rm pw} = 1$ ($q_{\rm br}(x,t) \to \exp(2\mathrm{i}x)$) as $t \to \pm\infty$, and may be generalized according to the invariant transformations listed in [28].

It is straightforward to see that in the case $\lambda \in \Re$ solution (15) tends to the periodical in time the Kuznetsov–Ma soliton when $\lambda > 1$; to the periodical in space, but not in time homoclinical orbit when $0 < \lambda < 1$ (the Akhmediev solution); and to the Peregrine solution [32] when $\lambda = 1$ (see examples on Fig. 3).

While evolving, the perturbations of the plane wave stay within the interval

$$|a_{\rm br} - a_{\rm pw}| \leqslant |q_{\rm br}| \leqslant |a_{\rm br} + a_{\rm pw}|, \tag{16}$$

where

$$a_{\rm br} = 2\cosh\psi\cos\eta, \quad \lambda = \frac{a_{\rm br}}{2} - \mathrm{i}\sin\eta\sinh\psi \quad \text{and} \quad v_{\rm br}^{-1} = 4\,\mathrm{Im}(\lambda)\frac{1+\coth^2\psi}{2} \tag{17}$$

(in our case $a_{\rm pw} = 1$). It was mentioned in [32], that the Ma-soliton tends to a usual envelope soliton solution of the NLS in the case when its amplitude is much larger. According to formula (16) the behaviour of the breathing wave (15) may be evidently interpreted as in some sense linear superposition of a nonlinear envelope with its own amplitude $a_{\rm br}$ and the plane wave with amplitude $a_{\rm pw}$.

A breather represents an interaction of an envelope soliton with the background. Let us now suppose that the soliton has run away from the region of interaction with the plane wave and is propagating over the zero background. Since the nonlinear spectrum λ is conserved, the breather's eigenvalue will be related to the envelope soliton parameters by (14). Comparing (17) with (14) one may conclude how the collision with a plane wave effects a soliton: the envelope preserves its amplitude in the interaction: $a_{\rm br} = a_{\rm sol}$, but it accelerates [33]. Value $v_{\rm br}^{-1}$ means dimensionless velocity in commoving (with the fundamental wave) references and then the results may be presented in a vivid way, see λ-plane on Fig. 3. Horizontal lines on the λ-plane show the equal amplitudes (their values are given by numbers); bent curves represent the equal-velocity lines (numbers indicate values $v_{\rm br}^{-1}$). The travelling solution feels the plane wave the less, the larger $a_{\rm sol}$ or/and the larger the difference between the speeds of the soliton and the plane wave is.

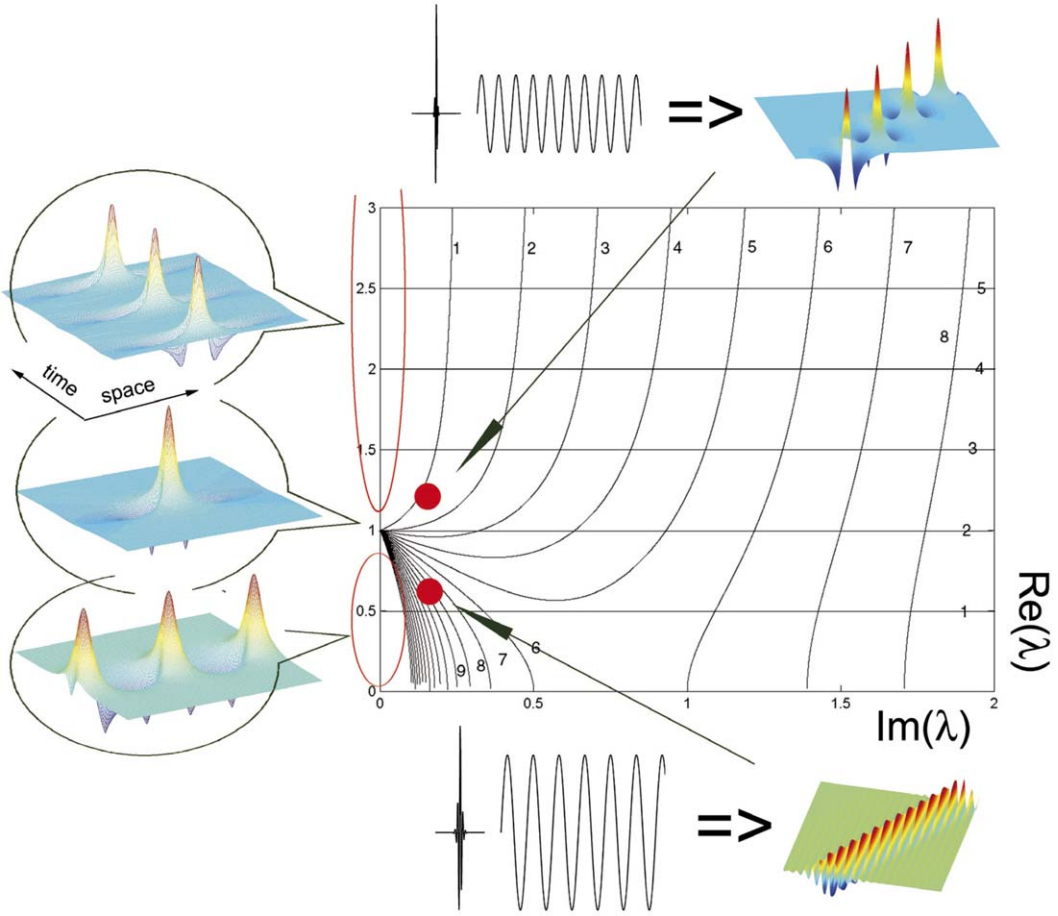

Fig. 3. λ-plane of a soliton over background and corresponding solutions. Left column of images, top–down: periodic in time the Kuznetsov–Ma solution ($\lambda > 1$), the limiting Peregrine solution ($\lambda = 1$), periodic in space the Akhmediev solution ($\lambda < 1$). Horizontal lines on the plane denote dimensionless soliton amplitude (numbers give values $a_{\rm sol} = a_{\rm br}$), bent curves show equal-velocity lines (numbers give values $v_{\rm br}^{-1}$).

If follows from formula (16), that when an envelope soliton interacts with a background plane wave, the maximum wave field is just the linear superposition of the amplitudes of the soliton and plane wave. The limiting Peregrine soliton corresponds to the case $a_{\rm sol}/a_{\rm pw} = 2$, and this is the maximum possible wave amplification that can be achieved in this process (3 times), although the amplification of the most unstable mode is about 2.4 [23].

Let us estimate the extreme wave amplitude that is achieved as the result of the soliton interaction (contained within the freak wave group) with the background waves. The determined soliton amplitude $A_{\rm s}$ gives the 'solitary part' of the freak wave (ratio $A_{\rm s}/A_{\rm fr}$ is given by the coloured part on Fig. 4, where $A_{\rm fr}$ is the maximum deviation of the surface from the zero level), the contribution of the background waves is given by $A_{\rm pw}$ ($A_{\rm pw} \approx H_{\rm s}/2$, ratio $A_{\rm pw}/A_{\rm fr}$ is given by shadows on Fig. 4). The rest (the white parts) estimate other effects. It is seen that often first two contributors may completely explain the registered wave amplitude, what proves the important role of the nonlinear modulation effect in the freak wave occurrence.

6. Numerical simulation of spatial evolution

The measuring device is typically installed at one point (in a fixed offshore platform or a buoy); and the provided information can tell nothing about the waves in the neighboring area. Simulation of the spatial wave evolution may complete the information. To perform such simulation one should make a supposition of unidirectional wave propagation and choose a model solving spatial evolution. Asymptotically derived evolution models are very convenient for this purpose, since may be easily transformed from temporal to spatial form; some of them also allow easy inversion

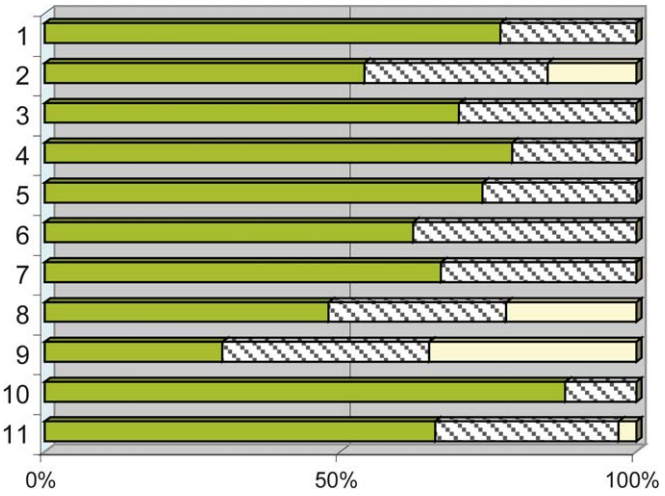

Fig. 4. 'Solitary parts' A_s (solid) and $H_s/2$ (shading) of the freak waves amplitude for records NA9711161053, NA9711180110, NA9711190751, NA9711191831, NA9711192011, NA9711192351, NA9711200131, NA9711200151, NA9711200311, NA9711200731 and the New Year Wave.

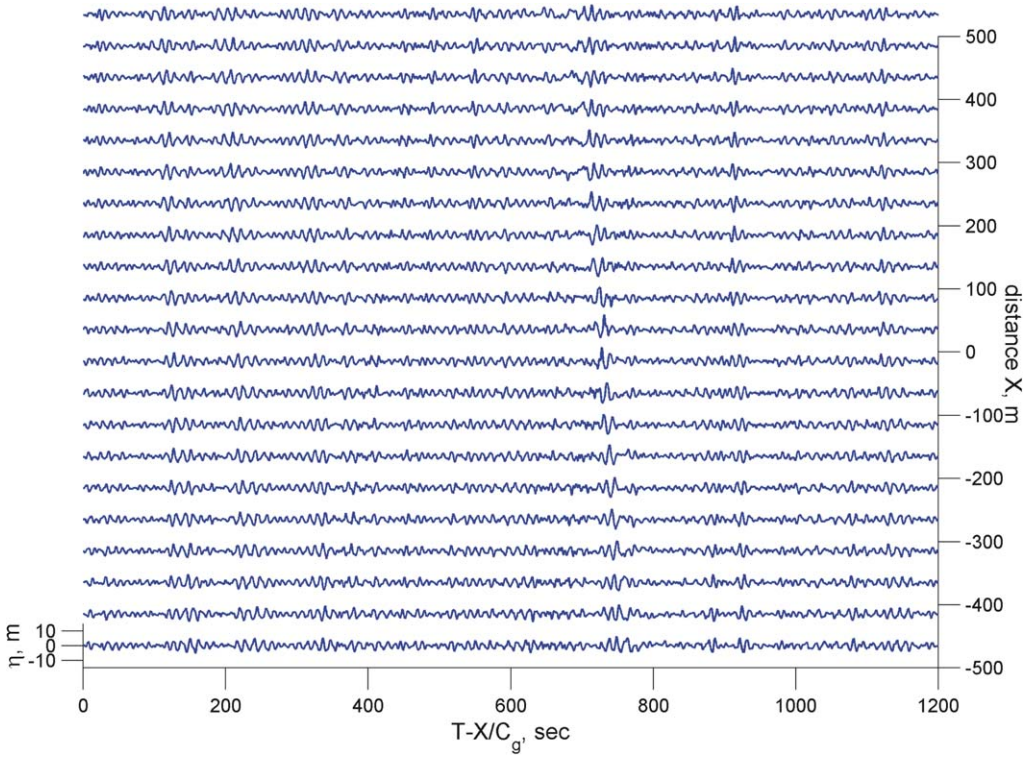

Fig. 5. Numerical simulations of wave record NA9711180110 within the frameworks of the Dysthe equation.

of the direction of evolution (they allow simulation of the backward wave propagation). The first numerical simulation of a freak wave record was probably conducted in [34] within the Dysthe model considering the New Year Wave. We have performed similar computations of the measured freak waves within different approximate models.

Figs. 5 and 6 demonstrate the wave evolution backward ($X < 0$) and forward ($X > 0$) wave propagation of two freak waves. It is computed within the framework of the Dysthe equation in the assumption of infinitively deep water (see [15] for details). The freak waves occur over intensive wave groups that are broader before and after the freak event. To estimate the freak wave lifetime T_{life} the abnormality index AI was computed at each distance following definition (1) (see Figs. 7 and 8, solid thick line). It is found out that a freak wave lives from several up to hundred

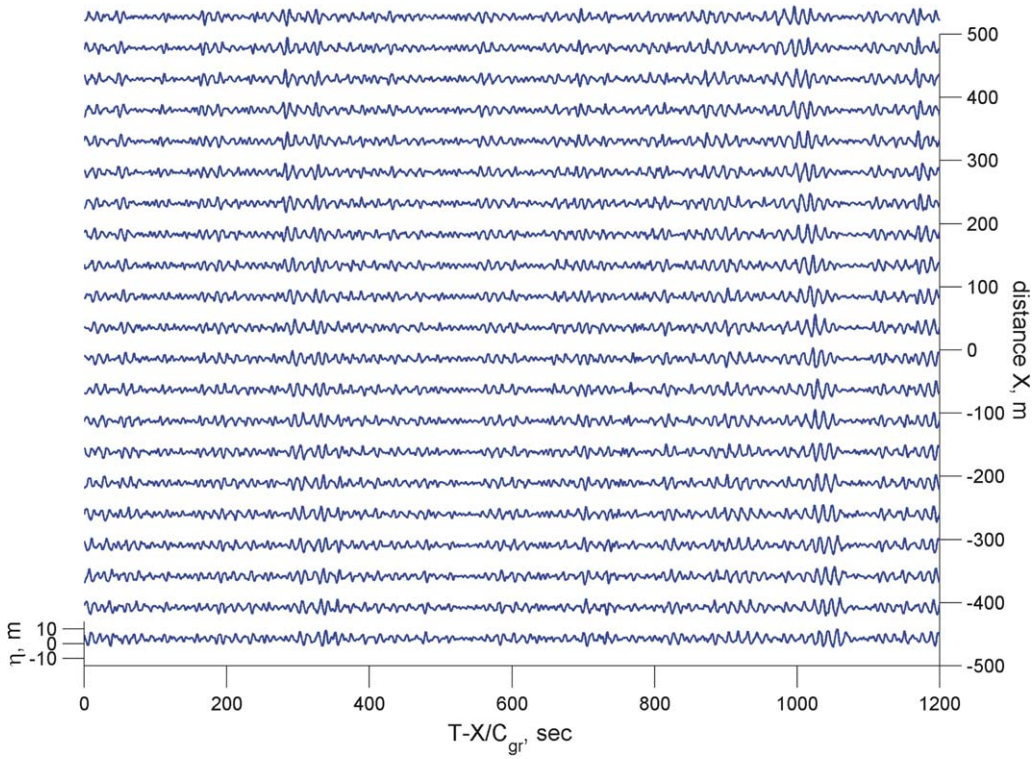

Fig. 6. Numerical simulations of wave record NA9711192011 within the frameworks of the Dysthe equation.

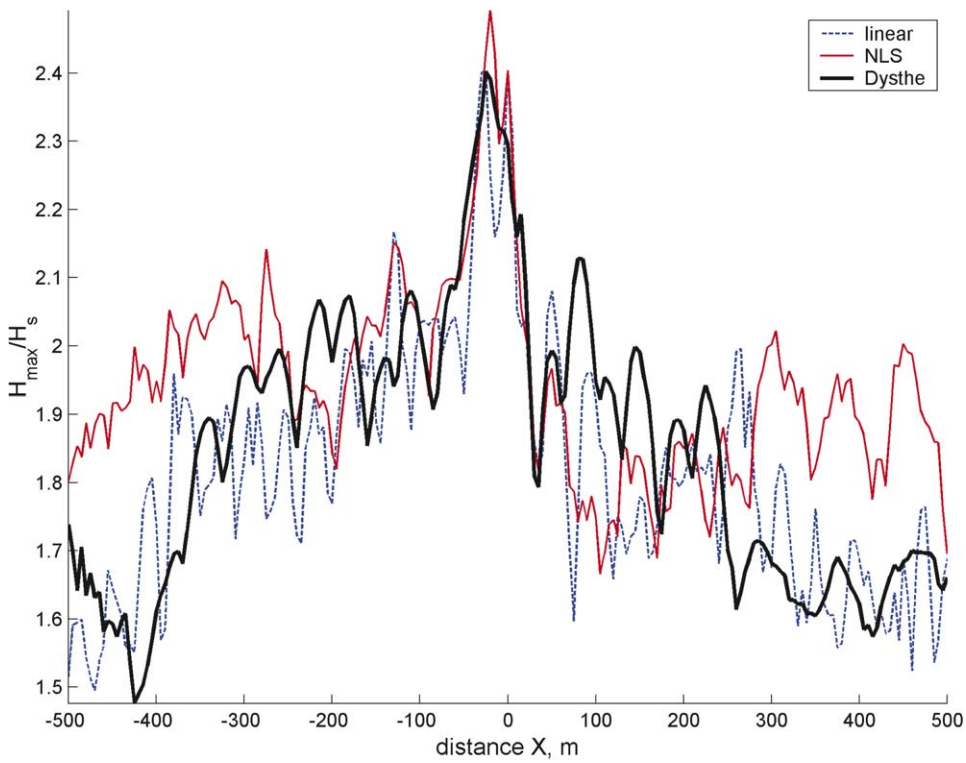

Fig. 7. Abnormality index computed on the basis of simulation displayed on Fig. 5 (record NA9711180110) (thick solid line) and comparison with the NLS model (thin solid line) and the linear limit (dashed).

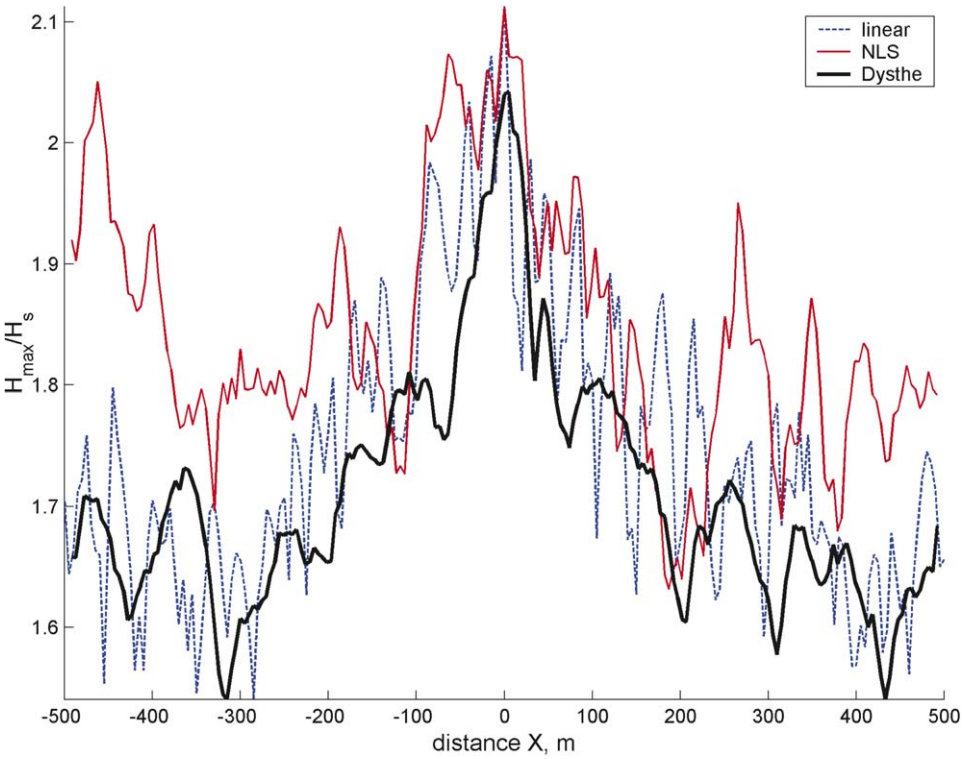

Fig. 8. Abnormality index computed on the basis of simulation displayed on Fig. 6 (record NA9711192011) (thick solid line) and comparison with the NLS model (thin solid line) and the linear limit (dashed).

seconds (what qualitatively agrees with observations), so the huge wave may make one or many oscillations during the freak wave occurrence. Similar simulations were also performed within the frameworks of the NLS equation (thin solid line on Figs. 7 and 8) and the linear limit (dashed line on Figs. 7 and 8). The peak value of AI at $X = 0$ for the Dysthe model on Figs. 7 and 8 is lower than the measured value because of the bandpass when initialising the computations, see [34]. This distinction shows contribution of high frequency waves to the freak wave event. On the other hand, the significant difference between the results of nonlinear simulations observed on Figs. 7 and 8 even for relatively small distances speaks about poor applicability of the weakly nonlinear models for the description of the measured time series. This is more distinctive when the freak wave contains a larger envelope soliton (i.e., I_{BF} is larger, the case of 'freak groups'). Following [35] one could expect reasonable agreement between the NLS and Dysthe theories at least up to 10 wavelengths (about 1400 m in our case) if the steepness is about 0.1, but the freak events are represented by steeper waves. This contradicts the desire to observe the action of the self-modulation (its typical scale is about 2 km in our case). In contrast to the Dysthe or linear models the NLS equation supports undying solitons that preserve their amplitudes and may generate freak waves again and again when the phase combination of the plane wave and background waves is successful.

We should actually remark that the peak height depends strongly on how successfully an individual wave is placed inside a group (otherwise on the phase of the wave). To demonstrate this effect Fig. 9 is given, where different definitions of wave amplification are used. First, the maximum wave height is defined as twice maximum amplitude (thin solid line), then it is defined as the maximum of the Hilbert envelope (dashed). AI is defined in the usual way and is given by the thick solid line on Fig. 9. It is quite evident, that the maximum amplification can be much higher if the phases of individual waves are slightly modified; the lifetimes of the freak waves may be much longer as well.

Another set of numerical experiments was conducted with "cancelled" nonlinearity. The field at the distance $X = -500$ (obtained from the simulations of the Dysthe model) was taken as the initial condition and computed forward to $X = 500$ within the framework of the linear theory. Typical dependence of maximum wave heights versus distance is given in Figs. 10 and 11 by dashed lines. Although the process does not entirely reproduce the results of the Dysthe model simulation (thick solid line), the wave enhancement is achieved even in this case of "cancelled"

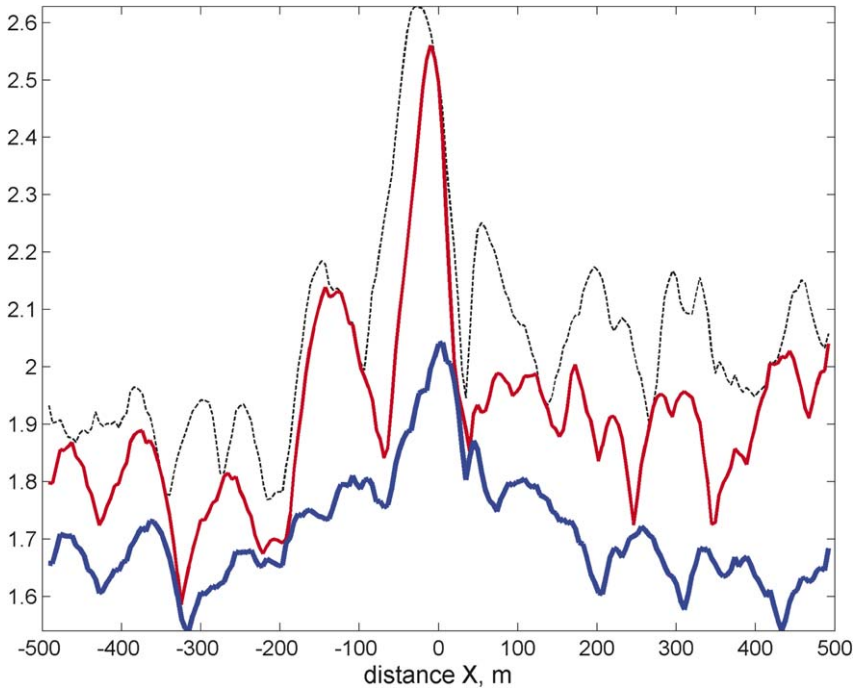

Fig. 9. Ratios $H_{\max}/H_{\mathrm{s}} = AI$ (thick solid line), $2A_{\max}/H_{\mathrm{s}}$ (thin solid line) and $2A_{\mathrm{Hilbert,max}}/H_{\mathrm{s}}$ (dashed) computed for the simulation displayed on Fig. 8; where $H_{\max}$ is the maximum height, $A_{\max}$ is the maximum amplitude of waves (maximum deviation from the zero level) and $A_{\mathrm{Hilbert,max}}$ is the maximum of modulus of the Hilbert transform.

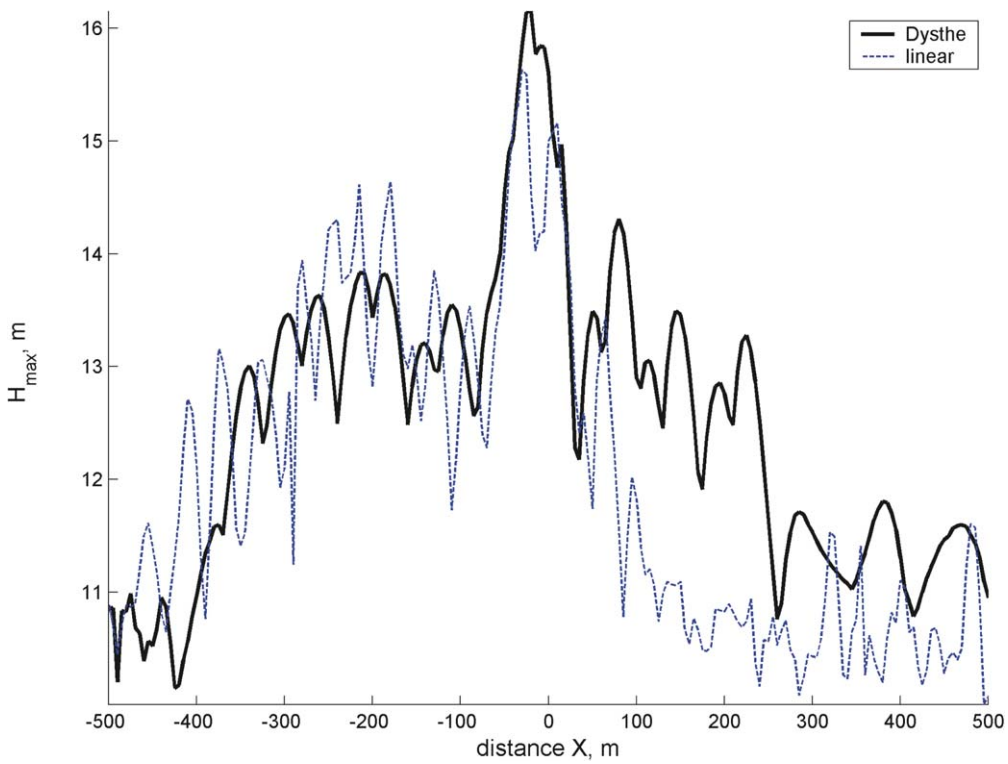

Fig. 10. Maximum wave height versus distance for record NA9711180110: comparison of the simulation in the Dysthe model (thick solid line) with the linear limit (dashed line). The initial conditions: field at position $X = -500$, computed within the frameworks of the Dysthe equation.

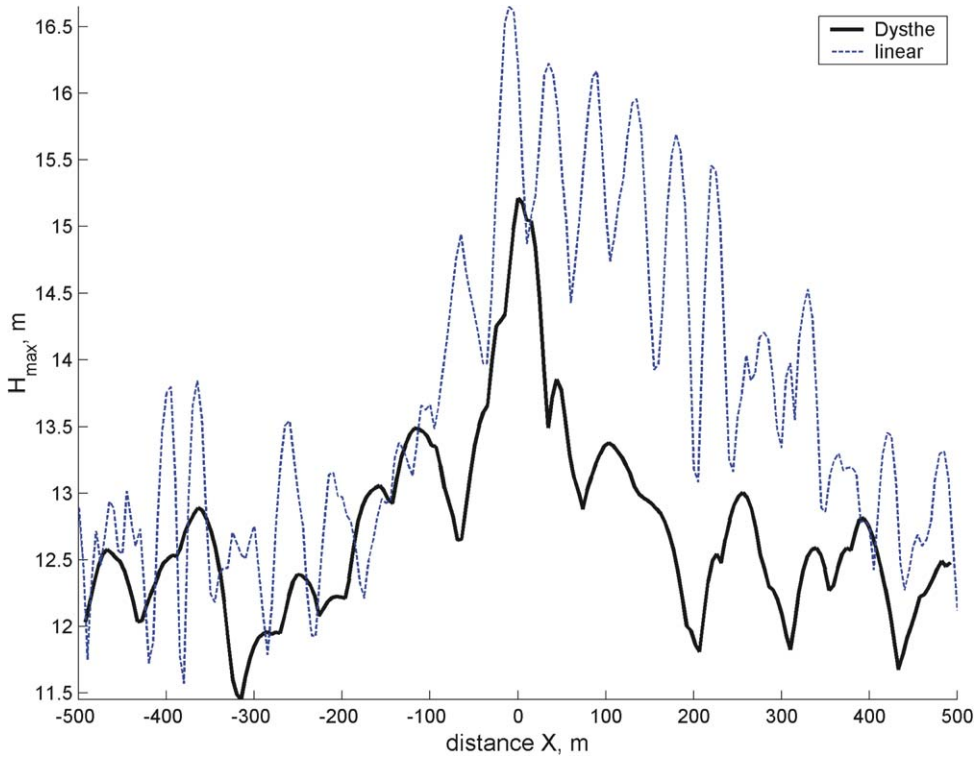

Fig. 11. Maximum wave height versus distance for record NA9711192011: comparison of the simulation in the Dysthe model (thick solid line) with the linear limit (dashed line). The initial conditions: field at position $X = -500$, computed within the frameworks of the Dysthe equation.

nonlinearity, what confirms the important role of dispersive effects. The formed intensive wave group apparently may then exceed the threshold of self-focusing and further amplify the wave due to the supplementary nonlinear exchange of energy within the group.

7. Conclusions

In the present paper a kind of summary of the author's recent research of measured freak waves is given. In our opinion a detailed study of measured freak wave events could make a short bridge to understand the phenomenon. The research is done with the help of well-established methods of wave record analysis, at the same time some new approaches are suggested. The most interesting, to our mind, is the application of the scattering problem of the nonlinear Schrodinger equation for the detecting envelope solitons and obtaining their parameters. In contrast to periodical statement of the problem we use a usual infinite-line approach and thus operate with solitons, but not with unstable modes. A clear idea about the dynamics of envelope solitons may then give a way to estimate and predict extreme wave conditions. Such comprehension is based upon the classical theory of soliton dynamics and the considered problem of a plane wave–envelope soliton interaction.

The conducted numerical simulations show that the measured freak waves remain intensive groups rather far out the moment of maximum growth. Thus, the considered freak waves do not appear 'from nowhere'. These groups dissolve with time if considered within the Dysthe model in contrast to the NLS equation predictions. The NLS solution thus will cause many freak waves, that turns out to be far from reality, and in fact changes the statistics. All the considered freak waves are, for the most part, solitary-like envelopes, what confirms the importance of self-modulational effects. On the other hand, simulations presented on Figs. 10 and 11 show that even linear approximation could eventually build huge waves.

The applicability of the Dysthe model for the simulation of the steep freak wave may be questioned. To moderate the deficiency we suggest considering extreme *envelope* properties (i.e.., *potential* wave amplification), instead of individual waves, since the shape of an envelope depends less on the phases of individual waves and may describe

a richer class of events, as it follows from Fig. 9. This may be more applicable for the case of "freak groups". Another important open problem consists in the ignorance of the transversal effects, although they may lead to new scenarios of a huge wave appearance [30,36]. The importance of wave directionality for the occurrence of freak waves may be supposed after observations of [37].

Acknowledgements

The author expresses his gratitude to E.N. Pelinovsky for valuable discussion and support; to B.V. Divinsky, S. Haver and C.G. Soares for the given records of freak waves and to the Institut de Recherche sur les Phenomenes Hors Equlibre and personally Ch. Kharif for the hospitality. I also thank the Reviewers for helping me improve this manuscript. The work is supported by grants INTAS 04-83-3032 and 03-51-4286, RFBR 05-05-64265 and the Russian Science Support Foundation.

References

[1] N. Mori, P.C. Liu, T. Yasuda, Analysis of freak wave measurements in the Sea of Japan, Ocean Eng. 29 (2002) 1399–1414.
[2] H. Chien, C.-C. Kao, L.Z.H. Chuang, On the characteristics of observed coastal freak waves, Coastal Eng. J. 44 (2002) 301–319.
[3] P. Stansell, Distributions of freak wave heights measured in the North Sea, Appl. Ocean Res. 26 (2004) 35–48.
[4] M. Onorato, A.R. Osborne, M. Serio, S. Bertone, Freak waves in random oceanic sea states, Phys. Rev. Lett. 86 (2001) 5831–5834.
[5] M. Onorato, A.R. Osborne, M. Serio, Extreme wave events in directional, random oceanic sea states, Phys. Fluids 14 (2002) L25–L28.
[6] P.A.E.M. Janssen, Nonlinear four-wave interactions and freak waves, J. Phys. Oceanogr. 33 (2003) 863–884.
[7] N. Mori, P.A.E.M. Janssen, On kurtosis and occurrence probability of freak waves, J. Phys. Oceanogr. (2005), submitted for publication.
[8] H. Socquet-Juglard, K.B. Dysthe, K. Trulsen, H.E. Krogstad, J. Liu, Probability distributions of surface gravity waves during spectral changes, J. Fluid Mech. 542 (2005) 195–216.
[9] E. Pelinovsky, A. Slunyaev, T. Talipova, A. Sergeeva, in: B.H. Choi, K.D. Suh, S.B. Yoon (Eds.), Mechanics of Freak Waves, Asian and Pacific Coasts 2005 (4–8 September, Jeju, Korea), Hanrimwon Publishing Co., Korea, 2005, pp. 67–78.
[10] D. Karunakaran, M. Bærheim, B.J. Leira, Measured and simulated dynamic response of a jacket platform, in: Proceedings of the 16th Symposium on Offshore Mechanics and Arctic Engineering, vol. II, ASME, 1997, pp. 157–164.
[11] K. Trulsen, K.B. Dysthe, Freak waves—a three-dimensional wave simulation, in: Proceedings of the 21st Symposium on Naval Hydrodynamics, National Academy Press, 1997, pp. 550–560.
[12] E.N. Pelinovsky, A.V. Slunyaev, T.G. Talipova, C. Kharif, Nonlinear parabolic equation and extreme waves on the sea surface, Radiophys. Quantum Electronics 46 (2003) 451–463.
[13] E. Pelinovsky, Ch. Kharif, A. Slunyaev, T. Talipova, A. Sergeeva, Freak waves: physical mechanisms and experimental data, in: Proc. Int. Conf. "Frontiers of Nonlinear Physics", Nizhny Novgorod, Russia, 2005, pp. 169–178.
[14] A. Slunyaev, E. Pelinovsky, C. Guedes Soares, Modeling freak waves from the North Sea, Appl. Ocean Res. 27 (2005) 12–22.
[15] A.V. Slunyaev, E.N. Pelinovsky, C. Guedes Soares, Analysis and simulation on freak waves in the North Sea, in: Proc. Int. Symp. "Topical Problems of Nonlinear Wave Physics", vol. NWP-3, 2005, pp. 102–103.
[16] B.V. Divinsky, B.V. Levin, L.I. Lopatukhin, E.N. Pelinovsky, A.V. Slyunyaev, A freak wave in the Black Sea: observations and simulation, Dokl. Earth Sci. A 395 (2004) 438–443.
[17] C. Kharif, E. Pelinovsky, Physical mechanisms of the rogue wave phenomenon, Eur. J. Mech. B Fluids 22 (2003) 603–634.
[18] V. Zakharov, Stability of periodic waves of finite amplitude on a surface of deep fluid, J. Appl. Mech. Tech. Phys. 2 (1968) 190–194.
[19] V.E. Zakharov, Dynamic modeling of surface waves, in: Proc. of Int. Symp. "Topical Problems of Nonlinear Wave Physics", vol. "Plenary Talks. Workshops", 2005, pp. 23–24.
[20] V.E. Zakharov, A.B. Shabat, Exact theory of two-dimensional self-focussing and one-dimensional self-modulation of waves in nonlinear media, Sov. Phys. JETP 34 (1972) 62–69.
[21] M.J. Ablowitz, D.J. Kaup, A.C. Newell, H. Segur, The inverse scattering transform – Fourier analysis for nonlinear problems, Stud. Appl. Math. 53 (1974) 249–315.
[22] A.R. Osborne, M. Petti, Laboratory-generated, shallow-water surface waves: Analysis using the periodic, inverse scattering transform, Phys. Fluids 6 (1994) 1727–1744.
[23] A.R. Osborne, M. Onorato, M. Serio, Nonlinear Fourier analysis of deep-water, random surface waves: Theoretical formulation and experimental observations of rogue waves, in: Proc. of Hawaiian Winter Workshop: Rogue Waves, 2005.
[24] A.L. Islas, C.M. Schober, Predicting rogue waves in random oceanic sea states, Phys. Fluids 17 (2005) 031701.
[25] C.A. van Duin, The effect of non-uniformity of modulated wavepackets on the mechanism of Benjamin–Feir instability, J. Fluid Mech. 399 (1999) 237–249.
[26] E.A. Kuznetsov, To the question of solitons in parametrically unstable plasma, Dokl. USSR 236 (1977) 575–577 (in Russian).
[27] Y.-Ch. Ma, The perturbed plane-wave solutions of the cubic Schrodinger equation, Stud. Appl. Math. 60 (1979) 43–58.
[28] K.B. Dysthe, K. Trulsen, Note on breather type solutions of the NLS as a model for freak-waves, Phys. Scripta T82 (1999) 48–52.
[29] A. Calini, C.M. Schober, Homoclinic chaos increases the likelihood of rogue wave formation, Phys. Lett. A 298 (2002) 335–349.
[30] A. Slunyaev, C. Kharif, E. Pelinovsky, T. Talipova, Nonlinear wave focusing on water of finite depth, Physica D 173 (2002) 77–96.

[31] M. Tajiri, Y. Watanabe, Breather solutions to the focusing nonlinear Schrodinger equation, Phys. Rev. E 57 (1998) 3510–3519.
[32] D.H. Peregrine, Water waves, nonlinear Schrodinger equations and their solutions, J. Austral. Math. Soc. Ser. B 25 (1983) 16–43.
[33] A.V. Slunyaev, Collision of an envelope soliton with a plane wave within the frameworks of the nonlinear Schrodinger equation, Proc. Acad. Eng. Sci. of Russian Federation 14 (2005) 41–46 (in Russian).
[34] K. Trulsen, Simulating the spatial evolution of a measured time series of a freak wave, in: M. Olagnon, G.A. Athanassoulis (Eds.), Proc. Workshop "Rogue Waves 2000", Brest, France, 2001, pp. 265–274.
[35] K. Trulsen, C.T. Stansberg, Spatial evolution of water waves: numerical simulation and experiment of bichromatic waves, in: Proc. Conference of the ISOPE, 2001, pp. 71–77.
[36] A.R. Osborne, M. Onorato, M. Serio, The nonlinear dynamics of rogue waves and holes in deep water gravity wave trains, Phys. Lett. A 275 (2000) 386–393.
[37] U.F. de Pinho, P.C. Liu, C.E.P. Ribeiro, Freak waves at Campos Basin, Brazil, Geofizika 21 (2004) 53–67.